

Synthesis and in Vitro Cytotoxicity Profile of the *R*-Enantiomer of 3,4-Dihydroxymethamphetamine (*R*-(-)-HHMA): Comparison with Related Catecholamines

Anne Felim,[†] Guadalupe Herrera,[‡] Anne Neudörffer,[†] Manuel Blanco,[‡]
José-Enrique O'Connor,^{*,‡} and Martine LARGERON^{*,†}

UMR 8638 CNRS, Université Paris Descartes, Synthèse et Structure de Molécules d'Intérêt Pharmacologique, Faculté des Sciences Pharmaceutiques et Biologiques, 4 Avenue de l'Observatoire, 75270 Paris cedex 06, France, and Laboratorio de Citómica, Unidad Mixta de Investigación CIPF-UVEG, Centro de Investigación Príncipe Felipe, Avenida Autopista del Saler 16, 46012 Valencia, Spain

Received September 16, 2009

(±)-3,4-Methylenedioxymethamphetamine (MDMA, also known as “ecstasy”) is a chiral drug that is essentially metabolized in humans through *O*-demethylenation into 3,4-dihydroxymethamphetamine (HHMA). There has recently been a resurgence of interest in the possibility that MDMA metabolites, especially 5-(*N*-acetylcystein-*S*-yl)-*N*-methyl- α -methyl-dopamine (designated as 5-NAC-HHMA), might play a role in MDMA neurotoxicity. However, the chirality of MDMA was not considered in previously reported in vivo studies because HHMA, the precursor of the 5-NAC-HHMA metabolite, was used as the racemate. Since the stereochemistry of this chiral drug needs to be considered, the first total synthesis of *R*-(-)-HHMA is reported. Using *L*-DOPA as the chiral source, the preparation of *R*-(-)-HHMA is achieved through seven steps, in 30% overall yield and 99.5% enantiomeric excess. The cytotoxicity of *R*-(-)-HHMA and related catecholamines has been further determined by flow cytometric analysis of propidium iodide uptake in human dopaminergic neuroblastoma SH-SY5Y cells and by an *Escherichia coli* plate assay, specific for the detection of oxidative toxicity. The good correlation between the toxicities observed in both systems suggests that SH-SY5Y cells are sensitive to oxidative toxicity and that cell death (necrosis) would be mediated by reactive oxygen species mainly generated from redox active quinonoid centers. In contrast, apoptosis was detected for 3,4-dimethoxymethamphetamine (MMMA), the synthetic precursor of HHMA possessing a protected catechol group. MMMA was not toxic in the bacterial assay, indicating that its toxicity is not related to increased oxidative stress. Finally, we can conclude that there is a need to distinguish the toxicity ascribed to MDMA itself, also bearing a protected catechol moiety, from that depending on MDMA biotransformation leading to catechol metabolites such as HHMA and the thioether conjugates.

Introduction

The alarming increase in the recreational use of (±)-3,4-methylenedioxymethamphetamine (MDMA, also known as “ecstasy”) and the multitude of adverse effects resulting from its misuse (1–5) require a complete understanding of the pharmacology and toxicology of this synthetic psychoactive drug. However, the precise mechanisms by which MDMA induces neurotoxic effects, both in laboratory animals (rodents, nonhuman primates) and humans, remain to be fully elucidated (6–11). MDMA-mediated neurotoxicity could be related to some of the adverse effects such as hyperthermia, the serotonin (5-HT) transporter action, 5-HT_{2A} agonism, glutamate excitotoxicity, the monoamine oxidase metabolism of dopamine and serotonin, and nitric oxide together with the formation of damaging peroxynitrite, and, importantly, the formation of MDMA neurotoxic metabolites (12). Among these factors, which may act collectively in a synergistic manner conducive to neurotoxicity, systemic metabolism of MDMA seems to be a crucial step (13–15).

In humans, MDMA is essentially metabolized through *O*-demethylenation into 3,4-dihydroxymethamphetamine (HHMA) (16). Because of its catechol moiety, HHMA can be easily oxidized to the corresponding *o*-quinone species, which exhibits a double reactivity. First, it can undergo redox-cycling which produces semiquinone radical and leads to the generation of reactive oxygen species (ROS). Second, it behaves as a highly electrophilic compound which can be conjugated with thiol nucleophiles such as glutathione or *N*-acetylcysteine (NAC) to form redox active catechol–thioether mono- and bis-conjugates (17) able to induce cytotoxicity mediated by ROS (18).

The potential role of metabolites in MDMA neurotoxicity has been a topic of recent interest (12, 17, 19). Among them, the catechol–thioether metabolite 5-(*N*-acetylcystein-*S*-yl)-*N*-methyl- α -methyl-dopamine (here designated as 5-NAC-HHMA) has been the most strongly implicated in MDMA neurotoxicity (20, 21). Studies have been recently performed to further assess the 5-HT neurotoxic potential of 5-NAC-HHMA, but the results are at odds with those previously reported and argue against a pivotal role for 5-NAC-HHMA in MDMA-induced 5-HT neurotoxicity (19). The reasons for this discrepancy is not clear, but it is important to note that 5-NAC-HHMA used in these studies was prepared through a biomimetic electrochemical oxidation process (18), whereas the procedure previously utilized

* Corresponding author. Tel: (+) 33 1 53 73 96 46. Fax: (+) 33 1 44 07 35 88. E-mail: eoconnor@ochoa.fib.es (J.E.O.C.); martine.largeron@parisdescartes.fr (M.L.).

[†] Université Paris Descartes.

[‡] Centro de Investigación Príncipe Felipe.

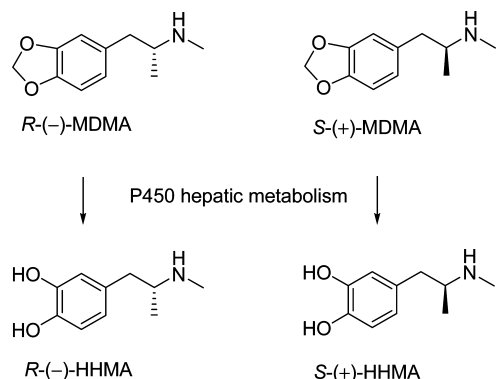


Figure 1. Stereochemistry of the hepatic metabolism leading to *R*(-)-HHMA and *S*(+)-HHMA.

for synthesizing this metabolite involved the oxidation of the catechol with mushroom tyrosinase (20), which yields a different ratio of 5-NAC-HHMA diastereoisomers (22). Consequently, for a comprehensive study on MDMA-induced neurotoxicity, the stereochemistry of the metabolism of this chiral drug needs to be considered (23).

MDMA is consumed as a racemate that is a 1:1 mixture of *R*(-)-MDMA and *S*(+)-MDMA enantiomers (Figure 1). Both enantiomers show different pharmacological and pharmacokinetic profiles (24–30). For most of the known psychomimetic agents having at least one chiral center, the most potent isomer exhibits the absolute *R* configuration (24). In the case of MDMA, the potency assignment is reversed since *S*(+)-MDMA has been shown to display effective psychomimetic properties in humans. Furthermore, although *R*(-)-MDMA has the higher affinity for the serotonin receptor 5-HT₂, the *S*(+)-MDMA isomer produces the most lasting 5-HT deficits that probably reflects its neurotoxicity (25). Metabolism could also contribute to differences between both enantiomers. Especially, the difference in their pharmacokinetic properties may be caused by enantioselective metabolism by cytochrome P450 isoenzymes, in particular CYP2D6 and CYP2C19 (23). Therefore, HHMA, which is a major MDMA metabolite in humans, exists also as a pair of enantiomers (30) (Figure 1). HHMA being the precursor of the thioether metabolites, these conjugates exist as a mixture of diastereoisomers as they possess several chiral centers: that of HHMA present in the alkylamino side chain (carbon atom α to the amine function), together with those present in the thiol moieties. Because MDMA enantiomers have different biological activities, it is of a great interest to study whether the catechol–thioether diastereoisomers of HHMA also exhibit dissimilar biological properties. The preparation of such diastereoisomers requires the previous synthesis of enantiomerically pure precursors *R*(-)-HHMA and *S*(+)-HHMA, which are more difficult to synthesize than the racemate. To circumvent this problem, analytical and semipreparative methodologies for the diastereoisomeric separation of MDMA thioether conjugates have been recently reported, but this separation method only furnished small quantities of both diastereoisomers (22).

This prompted us to envision the total synthesis of enantiomerically pure precursors, *R*(-)-HHMA and *S*(+)-HHMA. Starting from these compounds, it would be then easy to prepare the corresponding diastereomerically pure forms of thioether metabolites, either through the straightforward one-pot electrochemical synthesis we have recently reported for preparing diverse catechol–thioether mono- and bis-conjugates starting from (\pm)-HHMA racemate (18, 31) or by using the enzymatic procedure described by other investigators (20, 21, 32).

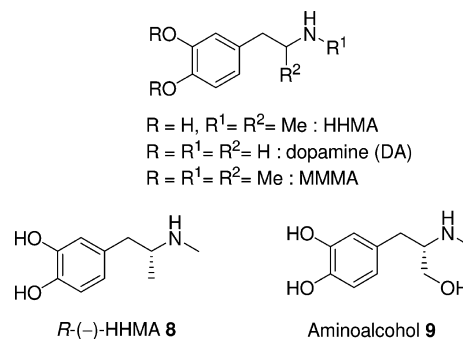


Figure 2. Chemical structures of studied compounds.

In this article, we report the first total synthesis of *R*(-)-HHMA in 30% overall yield and 99.5% enantiomeric excess (ee), using L-DOPA as the inducer of chirality. To the best of our knowledge, a sole synthesis of enantiomerically enriched *S*(+)-HHMA (80% ee) is known (33). Consequently, as long as the synthesis of optically pure *S*-enantiomer is not reported, the enantioselective toxicity of both enantiomers of HHMA cannot be addressed. Nevertheless, we have decided to examine the *in vitro* toxicity profile of *R*(-)-HHMA in a broader context, using different assays which could be predictive of the toxicological effects associated with catecholamine-type structures. The cytotoxicity of *R*(-)-HHMA and related catecholamines (Figure 2) has been assessed in human dopaminergic neuroblastoma SH-SY5Y cells. Flow cytometry has been used to discriminate between live, apoptotic, and necrotic cells and to measure the activity of caspase-3, an effector of apoptosis. In addition, the cytotoxicity observed in SH-SY5Y cells has been compared with that evaluated in an *Escherichia coli* plate assay which is specific for the detection of oxidative toxicity (34).

Experimental Procedures

Chemistry. All reagents and solvents (HPLC grade) were commercial products of the highest available purity and were used as supplied. Dopamine hydrochloride (DA, HCl) was purchased from Aldrich.

Analytical thin-layer chromatography was carried out on silica gel Macherey-Nagel Polygram SIL G/UV 254 (0.25 mm). Column chromatography was performed on Macherey-Nagel Si 60 M silica gel (40–63 μ m). Optical rotations were measured at 25 °C using a Perkin-Elmer 341 polarimeter. Melting points were measured on a Kofler apparatus.

HPLC was carried out using a Waters system consisting of a 600E multisolvent delivery system, a Rheodyne-type loop injector, and a 2487 dual-channels UV–visible detector set at 254 and 278 nm. A mixture of two solvents constituted the mobile phase: acetonitrile (MeCN) and solvent A. Solvent A was prepared by adding 1% concentrated trifluoroacetic acid (TFA) to deionized water. Semipreparative reversed-phase HPLC was performed using a 250 \times 20 mm, 5 μ m Kromasil C18 column and a 2 mL loop injector, whereas for the analytical reversed-phase HPLC, a 250 \times 4.6 mm, 5 μ m Kromasil C18 column, together with a 50 μ L loop injector, were used.

¹H NMR and ¹³C NMR spectra were performed on a Bruker AC-300 spectrometer operating at 300 and 75 MHz, respectively. Chemical shifts are expressed as δ units (part per million) downfield from TMS (tetramethylsilane). The measurements were carried out using the standard pulse sequences. The carbon type (methyl, methylene, methine, or quaternary) was determined by DEPT experiments. ¹H and ¹³C NMR spectra of all compounds are included in the Supporting Information as a proof of their identity.

High-resolution mass spectra (HRMS) were recorded on a LTQ-Orbitrap spectrometer operating in positive ion mode. (\pm)-3,4-

dihydroxymethamphetamine hydrobromide (HHMA, HBr) was synthesized in two steps from commercially available 3,4-dimethoxyphenylacetone using an adaptation of previously reported procedures with slight modifications (35–38).

(±)-3,4-Dimethoxymethamphetamine [(±)-MMMA]. (±)-MMMA was previously described as the hydrochloride salt (37, 38); 6.45 mL of a 40% aqueous solution of methylamine (8 equiv) were added dropwise to a solution of 3,4-dimethoxyphenylacetone (3.0 g, 15.45 mmol) in MeOH (50 mL) at 0 °C. The resulting solution was stirred under nitrogen at 0 °C for 30 min, and sodium borohydride (NaBH₄) (632 mg, 16.7 mmol) was added in small portions for 30 min. Then, the reaction mixture was allowed to warm at room temperature and stirred for 1 h. After the addition of K₂CO₃ (2.2 g), the solvent was evaporated under reduced pressure. H₂O (15 mL) was added to the residue, and the reaction mixture was extracted with diethyl ether (40 mL). The organic phase was then washed with 1 N HCl (15 mL). The resulting acidic aqueous phase was alkalized with K₂CO₃ and extracted with diethyl ether (50 mL). The organic phase was then dried over MgSO₄ and filtered off, and the solvent was evaporated. Column chromatography (dichloromethane–MeOH 80/20 v/v) afforded (±)-MMMA as a yellow oil (2.23 g, 10.65 mmol) in 69% yield. ¹H NMR (CDCl₃) δ 1.09 (d, *J* = 6.5 Hz, 3H), 1.44 (broad s, 1H), 2.41 (s, 3H), 2.62 (dd, *J* = 13.4 Hz, 2H), 2.77 (m, 1H), 3.88 (s, 3H), 3.89 (s, 3H), 6.75 (m, 2H), 6.83 (d, *J* = 8.1 Hz, 1H). ¹³C NMR (CDCl₃) δ 15.2, 30.4, 39.2, 55.8, 55.9, 57.0, 111.4, 112.1, 121.3, 128.0, 148.0, 149.2.

(±)-3,4-Dihydroxymethamphetamine hydrobromide (HHMA, HBr). A 48% aqueous solution of HBr (3.3 mL) (18.7 mmol) was added to (±)-MMMA (523 mg, 2.5 mmol). The resulting solution was heated to reflux for 1.5 h, under inert atmosphere. After the addition of 0.5 mL of methanol and evaporation under reduced pressure, the purple oil was purified by column chromatography (dichloromethane–MeOH 90:10 v/v) affording HHMA, HBr as a colorless oil (524 mg, 2.0 mmol) in 80% yield. Spectroscopic data were identical to those previously reported (38).

Methyl (S)-2-Amino-3-(3,4-dihydroxyphenyl)propanoate Hydrochloride (1). Thionyl chloride (6.57 mL, 90 mmol) was added dropwise to a solution of L-DOPA (1.97 g, 10 mmol) in MeOH (100 mL) at 0 °C. After 18 h at 20 °C, the solvent was evaporated giving amine chlorohydrate **1** in 100% yield (2.48 g) as a white solid; mp 95–96 °C (surprisingly, this value markedly differs from that previously reported in the literature (39) mp 174–175 °C); [α]_D²⁵ + 9.4 (*c* 0.03, MeOH); literature (39) [α]_D²⁵ + 7.9 (*c* 1.0, MeOH). Spectroscopic data were identical to those previously reported (39, 40).

Methyl (R)-2-(tert-Butoxycarbonylamino)-3-(3,4-dihydroxyphenyl)propanoate (2). Saturated aqueous NaHCO₃ (7.5 mL) and di-*tert*-butyl dicarbonate (Boc₂O) (1.25 g, 5.41 mmol) in THF (5.5 mL) were added to ester **1** (0.96 g, 3.87 mmol) in THF (7.5 mL), at 0 °C, under nitrogen. The resulting solution was allowed to warm to room temperature and stirred for 1 h. After acidification with 1 N HCl aqueous solution (12 mL), the solvent was evaporated, and the aqueous phase was extracted with ethyl acetate (40 mL). The organic phase was then dried over MgSO₄ and filtered off, and the solvent was evaporated under reduced pressure. Column chromatography (petroleum ether/ethyl acetate 60/40 v/v) afforded product **2** as a white solid (1.1 g, 3.53 mmol) in 92% yield. mp 138–139 °C; (literature (39) mp 134–135 °C); [α]_D²⁵ + 6.0 (*c* 0.1, MeOH); literature (39) [α]_D²⁵ + 6.9 (*c* 1.0, MeOH). Spectroscopic data were identical to those previously reported (39, 41).

Methyl (S)-2-(tert-Butoxycarbonylamino)-3-(3,4-dimethoxyphenyl)propanoate (3). To compound **2** (1.3 g, 4.2 mmol) in acetone (12 mL) were added MeI (2.1 mL, 33.6 mmol) and K₂CO₃ (5.8 g, 42.1 mmol). The reaction mixture was heated to reflux for 6 h. After filtration of the precipitate, the solution was concentrated, and the resulting residue was dissolved in diethyl ether (40 mL). The organic phase was then washed with water (20 mL), dried over MgSO₄, filtered off, and the solvent evaporated under reduced pressure. Column chromatography (petroleum ether/ethyl acetate 60/40 v/v) afforded product **3** as a white solid (1.41 g, 4.15 mmol)

in 99% yield. mp 78–79 °C; (literature (39) mp 77–78 °C); [α]_D²⁵ + 4.6 (*c* 0.05, MeOH); literature (39) [α]_D²⁵ + 6.0 (*c* 1.0, MeOH). Spectroscopic data were identical to those previously reported (39, 42, 43).

tert-Butyl [(S)-2-(3,4-Dimethoxyphenyl)-1-(hydroxymethyl)ethyl]-carbamate (4). Lithium aluminum hydride (LiAlH₄) solution in THF (1 M, 35.4 mL) was added dropwise to a solution of compound **3** (3 g, 8.84 mmol) in dry THF (40 mL). The reaction mixture was stirred under nitrogen at room temperature for 1 h. Then, 0.5 mL of ice–water and 0.5 mL of 0.5 M NaOH were successively added. The solid Al(OH)₃ was filtered off and washed with dichloromethane (2 × 40 mL). The filtrate was concentrated to dryness, and the residue was dissolved in dichloromethane (40 mL). The resulting organic phase was then washed with water (20 mL), dried over MgSO₄, filtered off, and then concentrated. Column chromatography (petroleum ether/ethyl acetate 60/40 v/v) afforded N-protected α-aminoalcohol **4** as a white solid (2.5 g, 8.0 mmol) in 90% yield. mp 94–95 °C; (literature (39) mp 91–92 °C); [α]_D²⁵ –19.0 (*c* 0.01, MeOH); literature (39) [α]_D²⁵ –19.6 (*c* 0.3, MeOH). Spectroscopic data were identical to those previously reported (39, 42, 43).

(S)-2-(tert-Butoxycarbonylamino)-3-(3,4-dimethoxyphenyl)-1-(4-methylbenzenesulfonyloxy) Propane (5). To a solution of α-aminoalcohol **4** (2.34 g, 7.51 mmol) in dichloromethane (15.5 mL) dried over CaCl₂ were added triethylamine (1.57 mL, 11.27 mmol), *p*-toluenesulfonyl chloride (1.72 g, 9.01 mmol), and dimethylaminopyridine (DMAP) (918 mg, 0.750 mmol). After stirring for 18 h at room temperature, under nitrogen, the reaction mixture was diluted with dichloromethane (40 mL). The organic phase was then washed with water (20 mL), dried over MgSO₄, and filtered off, and the solvent was evaporated under reduced pressure. The crude residue was recrystallized from the diethyl oxide/dichloromethane mixture affording compound **5** as a white solid (2.94 g, 6.3 mmol) in 84% yield. mp 155–156 °C; (literature (44) mp 146–148 °C); [α]_D²⁵ –16.2 (*c* 0.09, MeOH); literature (44) [α]_D²⁵ –15.4 (*c* 0.36, CHCl₃). ¹H NMR (CDCl₃) δ 1.41 (s, 9H), 2.47 (s, 3H), 2.80 (m, 2H), 3.87 (s, 6H), 3.95 (m, 2H), 4.73 (d, *J* = 7.0 Hz, 1H), 6.64 (d, *J* = 7.9 Hz, 1H), 6.71 (s, 1H), 6.74 (d, *J* = 7.9 Hz, 1H), 7.36 (d, *J* = 8.2 Hz, 2H), 7.78 (d, *J* = 8.2 Hz, 2H). ¹³C NMR (CDCl₃) δ 21.7, 28.3, 36.7, 50.8, 55.9 (×2), 69.9, 79.8, 111.2, 112.3, 121.3, 128.0, 129.1, 130.0, 132.5, 145.1, 147.8, 149.0, 155.0.

(R)-3,4-Dimethoxymethamphetamine (6) and (S)-3-(3,4-dimethoxyphenyl)-2-(*N*-methylamino)-propan-1-ol (7). LiAlH₄ solution in THF (1 M, 4.45 mL) was added dropwise to a solution of compound **5** (501 mg, 1.08 mmol) in dry dichloroethane (13.5 mL) at 0 °C. The resulting solution was allowed to warm to room temperature, under nitrogen, and stirred for 45 min. Then, the reaction mixture was heated to reflux for 1.5 h. After hydrolysis with 0.5 mL of ice–water and 0.5 mL of 0.5 M NaOH, the solid Al(OH)₃ was filtered off and washed with dichloromethane (2 × 40 mL). The filtrate was concentrated to dryness. Column chromatography of the residue (dichloromethane/methanol 95/5 v/v with 1.5% triethylamine) afforded compounds **6** (134.5 mg, 0.64 mmol) and **7** (31 mg, 0.15 mmol) as colorless oils in 60% and 13% yields, respectively.

Compound **6**: ¹H NMR (CDCl₃) δ 1.02 (d, *J* = 6.2 Hz, 3H), 2.02 (broad s, 1H), 2.34 (s, 3H), 2.57 (m, 2H), 2.70 (m, 1H), 3.81 (s, 3H), 3.82 (s, 3H), 6.69 (m, 2H), 6.76 (d, *J* = 8.7 Hz, 1H). ¹³C NMR (CDCl₃) δ 19.5, 33.9, 43.0, 55.8 (×2), 56.3, 111.1, 112.3, 121.1, 131.9, 147.4, 148.7. HRMS (ESI) *m/z* calcd for [M + H]⁺ 210.2955; found, 210.1489. [α]_D²⁵ –1.9 (*c* 0.06, MeOH).

Compound **7**: ¹H NMR (CDCl₃) δ 2.3 (m, 3H), 2.42 (s, 3H), 3.37 (dd, *J* = 10.8 Hz, 1H), 3.63 (dd, *J* = 10.8 Hz, 1H), 3.85 (s, 3H), 3.86 (s, 3H), 6.74 (m, 2H), 6.82 (d, *J* = 8.1 Hz, 1H). ¹³C NMR (CDCl₃) δ 33.7, 37.1, 55.9 (×2), 61.9, 62.0, 111.3, 112.2, 121.1, 131.0, 147.5, 148.9. HRMS (ESI) *m/z* calcd for [M + H]⁺ 226.2949; found, 226.1438. [α]_D²⁵ + 10.1 (*c* 0.01, MeOH).

(R)-3,4-Dihydroxymethamphetamine Hydrobromide HHMA, HBr (8). A 48% aqueous solution of HBr (2.6 mL) (15 mmol) was added to compound **6** (420 mg, 2 mmol). The resulting solution was heated to reflux for 1.5 h, under nitrogen. After the addition

of 0.5 mL of methanol and evaporation under reduced pressure, the orange oil was purified by column chromatography (dichloromethane/methanol 80/20) affording compound **8** as a colorless oil (376.5 mg, 1.44 mmol) in 72% yield. $[\alpha]_D^{25}$ -2.4 (c 0.05, MeOH). $^1\text{H NMR}$ (D_2O) δ 1.16 (d, $J = 6.6$ Hz, 3H), 2.57 (s, 3H), 2.68 (dd, $J = 13.9$ Hz, 1H), 2.80 (dd, $J = 13.9$ Hz, 1H), 3.35 (m, 1H), 6.62 (dd, $J = 1.9$ and 8.1 Hz, 1H), 6.71 (s, $J = 1.9$ Hz, 6.79 (d, 1H, $J = 8.1$ Hz). $^{13}\text{C NMR}$ (D_2O) δ 14.8, 29.9, 37.9, 56.4, 116.2, 116.9, 121.7, 128.1, 143.0, 143.9. HRMS (ESI) m/z calcd for $[\text{M} + \text{H}]^+$ 182.2419; found, 182.1175.

(S)-3-(3,4-Dihydroxyphenyl)-2-(N-methylamino)propan-1-ol Hydrobromide (9). The previous method, replacing compound **6** by compound **7** (414 mg, 2 mmol), afforded after column chromatography, compound **9** as a colorless oil (400.5 mg, 1.44 mmol) in 72% yield. $[\alpha]_D^{25}$ $+2.1$ (c 0.016, MeOH). $^1\text{H NMR}$ (D_2O) δ 2.62 (s, 3H), 2.74 (dd, $J = 14.2$ Hz, 1H), 2.83 (dd, $J = 14.2$ Hz, 1H), 3.37 (m, 1H), 3.53 (dd, $J = 12.3$ Hz, 1H), 3.73 (dd, $J = 13.6$ Hz, 1H), 6.64 (dd, $J = 1.9$ and 8.1 Hz, 1H), 6.73 (s, $J = 1.9$ Hz, 1H), 6.77 (d, $J = 8.1$ Hz, 1H). $^{13}\text{C NMR}$ (D_2O) δ 30.0, 32.5, 57.8, 61.0, 116.4, 116.9, 121.7, 127.8, 143.1, 144.1. HRMS (ESI) m/z calcd for $[\text{M} + \text{H}]^+$ 198.2413; found, 198.1122.

Cell Culture. Human neuroblastoma SH-SY5Y cells were obtained from the European Collection Cell Cultures (ECACC no. 94030304; Salisbury, UK). Cells were cultured in Dulbecco's modified Eagle's medium (DMEM) containing 15% fetal bovine serum (FBS), 1% nonessential amino acids, 2 mM L-glutamine, 100 IU/mL penicillin, and 100 $\mu\text{g}/\text{mL}$ streptomycin.

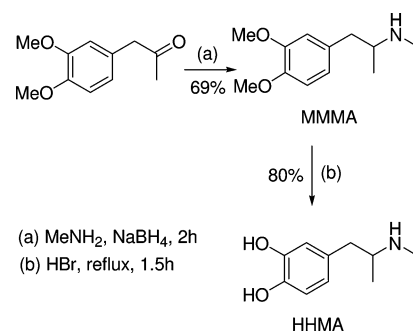
Flow Cytometry. For cell analysis, we used a Cytomics FC500 MPL multiwell-plate flow cytometer (Beckman-Coulter, Brea, CA), equipped with an air-cooled argon-ion laser tuned at 488 nm (blue light). To assay cell death, SH-SY5Y cells were seeded in plastic 96-well plates (final concentration in well 2.7×10^4 cells) and incubated in 10% FBS containing medium for 24 h (50% confluence) in a CO_2 incubator at 37 °C. Then, the indicated concentrations of the compounds in 5% FBS containing medium were added and the plates kept for further 24 h. Cells were then trypsinized and resuspended in their original wells in 5% FBS containing medium, in the presence of 2.5 $\mu\text{g}/\text{mL}$ propidium iodide (PI). To identify PI uptake by dead cells (PI positive) by flow cytometry, cells were excited at 488 nm, and emission was detected at 625 nm. From dose-response curves of at least three experiments, TC_{50} , the molar concentration producing 50% of cell death, was calculated. SDs at doses in the vicinity of the TC_{50} values were lower than 10%. The percentage of viable (PI negative), apoptotic (PI intermediate), and necrotic (PI positive) cells was calculated by means of a plot correlating cell size (forward-angle light scatter) and PI uptake (45).

To measure the mitochondrial generation of superoxide, trypsinized cells were resuspended in their original wells in 5% FBS containing medium in the presence of 1.25 μM MitoSOX Red probe (Invitrogen), a mitochondrial superoxide indicator having excitation/emission maxima of approximately 510/580 nm. The mean fluorescence intensity was calculated for each sample. The results were expressed as Fluorescence Arbitrary Units (F.A.U.). As a positive control, we used the superoxide generator plumbagin (2-methyl-5-hydroxy-1,4-naphthoquinone), inducing a mean intensity of 20 FAU at the dose of 0.02 mM.

Caspase-3 activity was measured by flow cytometry, using Cleaved Caspase-3 (Asp-175) Antibody (Alexa Fluor 488 Conjugate) in accordance with the protocol supplied by the manufacturer (Cell Signaling Technology). As a positive control, we used camptothecin inducing 54% of caspase-3 activity in SH-SY5Y cells at the dose of 0.5 μM (24 h).

Escherichia coli Cytotoxicity Plate Assays. The *E. coli* strains were IC5282 (OxyR⁺ strain), IC5204, deficient in the OxyR function (OxyR⁻ strain), and IC2880, a tryptophan-requiring strain (J8). Overnight cultures were grown in Oxoid Nutrient Broth No. 2. Solid minimal E4 medium contained 15 g of Difco agar and 4 g of glucose per liter of Vogel-Bonner E buffer (containing $\text{MgSO}_4 \cdot 7\text{H}_2\text{O}$ (10 g), citric acid monohydrate (100 g), K_2HPO_4 (500 g), and $\text{NaNH}_4\text{PO}_4 \cdot 7\text{H}_2\text{O}$ (175 g) per liter of distilled water). Top agar

Scheme 1. Two Step Synthesis of (\pm)-HHMA

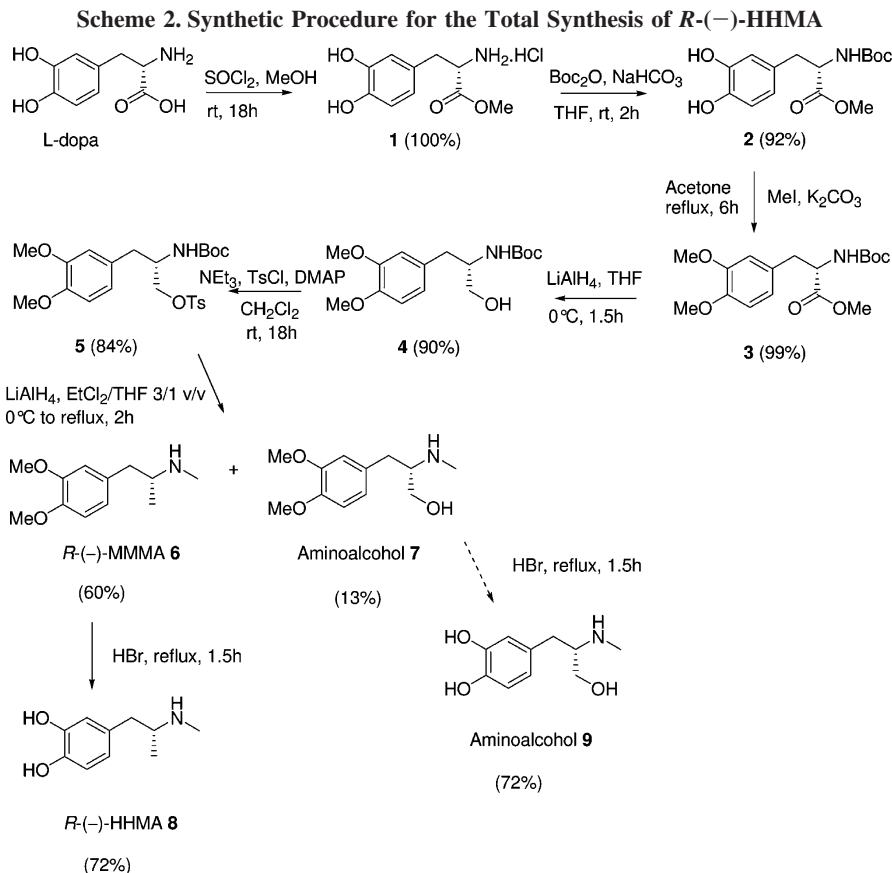


contained 6 g of Difco agar and 5 g of NaCl per liter of distilled water. In the assays, 100 μL of a suitable dilution of the test compound was added to 100 μL of the bacterial mix, containing approximately 800 test cells (from IC5282 or IC5204 strains) and 3×10^7 filler cells (from IC2880 strain) unable to grow in minimal E4 medium because of their requirement for tryptophan and used to obtain a background lawn. Where indicated, mushroom tyrosinase (EC 1.14.18.1; Sigma) was added to the assay (100 μL of a suitable dilution from a starting solution in 0.1 M sodium phosphate at pH 7.0). After the addition of 2.5 mL of molten top agar, the mixture was poured on plates containing solid E4 medium (about 35 mL), which were incubated at 37 °C, for 24 or 48 h. Data were the mean of at least three experiments. From the dose-response curves, the TC_{50} value was calculated as the concentration ($\mu\text{mol}/\text{plate}$) needed to reduce the survival to 50%. SDs at doses close to the TC_{50} values were lower than 10%.

Results and Discussion

Chemistry. Synthesis of (\pm)-HHMA. (\pm)-HHMA was prepared in a straightforward manner (Scheme 1), starting from commercially available 3,4-dimethoxyphenylacetone by reductive amination with sodium borohydride leading to (\pm)-MMMA in 69% yield. Complete demethylation of (\pm)-MMMA using hydrobromic acid, heated at reflux, afforded (\pm)-HHMA in 80% yield. Interestingly, this two step reaction sequence produced (\pm)-HHMA in a markedly improved overall yield (55%) when compared with that of earlier reported procedures starting from 3,4-dimethoxybenzaldehyde and nitroethane, for which the overall yields did not exceed 20% (35–38).

Synthesis of R(-)-HHMA. We prepared R(-)-HHMA from commercially available L-DOPA, chosen as the chiral source, through a seven step sequence which involved protection and deprotection reactions as reported in Scheme 2. This strategy required the intermediary synthesis of N-protected α -amino alcohol **4**, which has been previously described in four steps and 74.5% overall yield (39). Minor modifications of this procedure (solvent especially) allowed us to improve the yield in N-protected α -amino alcohol **4**, which was prepared in 82% overall yield. Quantitative esterification of L-DOPA in MeOH, followed by protection of the resulting amino group by treatment with di-*tert*-butyl-dicarbonate (Boc_2O) in THF, gave access to compound **2** in 92% yield. Methylation of the aromatic hydroxyl groups in acetone led, in quantitative yield, to compound **3** whose ester function was finally reduced with LiAlH_4 in THF, affording N-protected α -amino alcohol **4** in 90% yield. Treatment of **4** with *para*-toluenesulfonyl chloride (TsCl), in the presence of dimethylaminopyridine (DMAP) as the catalyst, provided the rather unstable tosylate **5** in 84% yield. Because **5** spontaneously converted through intramolecular cyclization between its alcohol group and its carbamate function to oxazolidinone on silica gel (39), tosylate **5** had to be purified by recrystallization. Concomitant reduction of the tosyl and



BOC groups was achieved using LiAlH_4 in dichloroethane/THF 3/1 v/v, leading to *R*-(-)-MMMA **6** as the major product (60%), with high optical purity (>99%) as determined by HPLC analysis of the mixture of Mosher amides prepared from racemate (\pm)-MMMA and from enantiomerically pure *R*-(-)-MMMA **6** (Figures 3 and 4). (See the Supporting Information for the synthesis of the Mosher amides.) Aminoalcohol **7** was also obtained as the minor product in 13% yield. Obviously, this reduction reaction proved to be the more difficult step of the synthetic procedure because of the occurrence of both the spontaneous cyclization of **5** to oxazolidinone and the partial reduction of the tosyl group to aminoalcohol **7**. Therefore, a thorough control of temperature was necessary to obtain good yields in *R*-(-)-MMMA **6**. Finally, complete demethylation of *R*-(-)-MMMA **6**, using hydrobromic acid heated at reflux, afforded *R*-(-)-HHMA **8** in 72% yield with 99.5% ee, whereas that of aminoalcohol **7** led to the deprotected α -aminoalcohol **9** in 72% yield.

Toxicological Study. The *in vitro* toxicological study was performed using the human dopaminergic neuroblastoma SH-SY5Y cell line, which is commonly used for studying the toxicity of catecholamine derivatives (46, 47). Loss of cell viability was monitored by flow cytometric analysis of propidium iodide (PI) uptake in dead cells (PI positive cells) having defective plasma membranes. In addition, as we previously determined the cytotoxicity profile of (\pm)-HHMA in *Escherichia coli* assays, specific for the detection of oxidative toxicity (18, 34), these bacterial tests were also included in the present study.

The results of the flow cytometric analysis of acute (24 h) cytotoxicity in SH-SY5Y cells are shown in Table 1. *R*-(-)-HHMA enantiomer **8** induced a decrease in cell viability similar to that resulting from exposure to the (\pm)-HHMA racemate, with a TC_{50} value of 0.30 mM. This decrease was also close to

that found for the control catecholamine dopamine (DA) ($\text{TC}_{50} = 0.25$ mM), whereas a lower toxicity ($\text{TC}_{50} = 1.0$ mM) was observed for aminoalcohol **9** isolated as a byproduct from the synthesis of *R*-(-)-HHMA **8** (Scheme 2). For the (\pm)-MMMA racemate, an intermediate in the synthesis of (\pm)-HHMA possessing a protected catechol group (Scheme 1) utilized for comparative purposes, toxicity was detected at high doses ($\text{TC}_{50} = 11.3$ mM). Similarly, MDMA metabolite 4-hydroxy-3-methoxymethamphetamine [(\pm)-HMMA] has been described as considerably less toxic than catechol-containing metabolites to PC12 cells, in the MTT reduction assay (38). Our results on cytotoxicity obtained from the PI uptake assay directly correlated with the extent of cell death evaluated by the MTT reduction assay (data not shown).

E. coli based assays allow a mechanistic characterization of toxicity so that they can be used as a model system. In these assays, toxicity mediated by ROS (ROS-TOX) can be detected in OxyR^- cells deficient in OxyR function because they are unable to exert antioxidant defenses (34, 48). In contrast, ROS-TOX is inhibited in OxyR^+ cells because of the elimination of hydrogen peroxide by catalase and alkylhydroperoxide reductase, both enzymes encoded by OxyR -regulated genes, so that the toxicity arising from the binding of quinones with cellular nucleophiles could then be shown (48, 49). The results of the *E. coli* plate assays are shown in Table 1. *R*-(-)-HHMA **8** and (\pm)-HHMA gave similar positive responses in the OxyR^- assay, with TC_{50} values of 0.8 and 0.75 $\mu\text{mol}/\text{plate}$, respectively, indicating high ROS-TOX induction. Furthermore, an increase in ROS-TOX ($\text{TC}_{50} = 0.6$ and 0.5 $\mu\text{mol}/\text{plate}$, respectively) was observed in the presence of tyrosinase, which catalyzed the oxidation to *o*-quinone. For (\pm)-MMMA, ROS-TOX induction was abolished, whereas for aminoalcohol **9** and dopamine, it was poor ($\text{TC}_{50} \approx 4$ $\mu\text{mol}/\text{plate}$) but greatly increased following catalytic oxidation by tyrosinase ($\text{TC}_{50} \approx 2$ $\mu\text{mol}/\text{plate}$). The

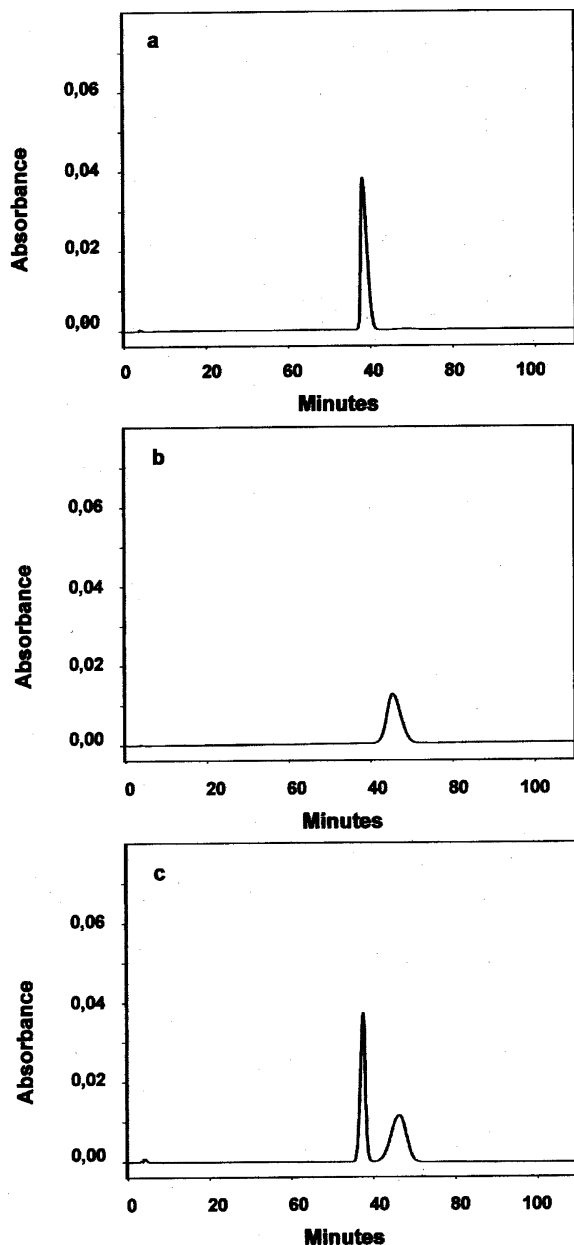


Figure 3. HPLC chromatograms for the analytical resolution of Mosher amide diastereoisomers prepared from (\pm)-MMMA racemate [(H₂O + 1%TFA)/MeCN 53/47; flow rate, 0.9 mL·min⁻¹]: (a) Mosher amide of *R*-(-)-MMMA isolated after semipreparative HPLC; (b) Mosher amide of *S*-(+)-MMMA isolated after semipreparative HPLC; (c) mixture of the Mosher amides obtained from (\pm)-MMMA racemate.

enhancement of toxicity promoted by tyrosinase suggests that the oxidation of these catecholamines to the corresponding *o*-quinone opens the way for redox cycling, leading to the formation of ROS (18). In contrast, the negative response in the OxyR⁺ assay (Table 1), even in the presence of tyrosinase (data not shown), was indicative of the absence of quinone-promoted toxicity, which is resistant to inhibition by antioxidant defenses (48, 49).

The good correlation found between the toxicity observed in SH-SY5Y cells and in *E. coli* OxyR⁻ cells would indicate a susceptibility of the SH-SY5Y cell line to the oxidative toxicity induced by the catecholamine derivatives. Consistent with this possibility is the mitochondrial generation of superoxide anion by these compounds in SH-SY5Y cells, detected by flow cytometric analysis using the MitoSOX Red fluorochrome (Table 2). Note, however, that HHMA and DA induced similar

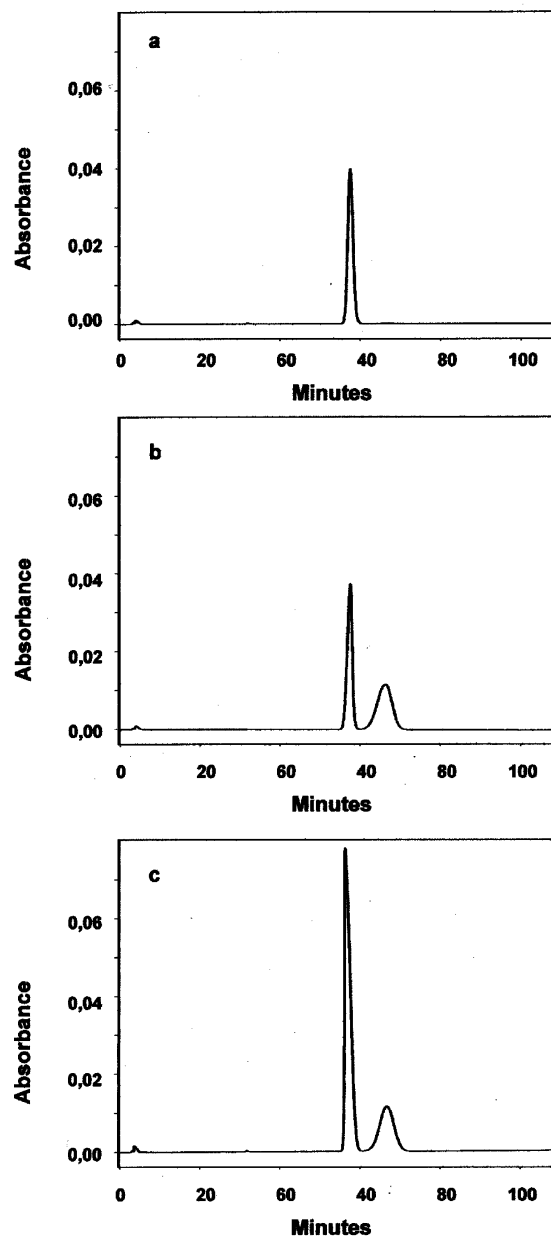


Figure 4. HPLC chromatograms for the analytical determination of the enantiomeric excess of *R*-(-)-MMMA 6 [(H₂O + 1%TFA)/MeCN 53/47; flow rate, 0.9 mL·min⁻¹]: (a) Mosher amide prepared from enantiomerically pure *R*-(-)-MMMA 6; (b) mixture of the Mosher amides obtained from (\pm)-MMMA racemate. (c) Mosher amide prepared from enantiomerically pure *R*-(-)-MMMA 6 together with the mixture of Mosher amides obtained from (\pm)-MMMA racemate.

toxicities in SH-SY5Y cells, whereas, converse to HHMA, DA was found to be a poor inducer of ROS-TOX in *E. coli* OxyR⁻ cells (Table 1).

Flow cytometry offers the possibility of multiparametric assays simultaneously providing several end points to characterize different modes of cell death at a single-cell level (45). In addition to the assay of plasma membrane permeability (PI uptake) for cell death evaluation (TC₅₀ value), we used flow cytometry to discriminate between live (PI negative), apoptotic (PI intermediate), and necrotic (PI positive) subpopulations, by means of a plot correlating cell size (forward-angle light scatter) and PI uptake (Table 3). For *R*-(-)-HHMA, (\pm)-HHMA, aminoalcohol 9, and DA induction of necrotic cells but not that of apoptotic cells was detected. In contrast, induction of apoptotic cells (48% at 10 mM) was clearly observed for (\pm)-

Table 1. In Vitro Cytotoxicity Profile of *R*-(-)-HHMA in Comparison with Related Catecholamines

compound	TC ₅₀ in Assay			
	SH-SY5Y ^a	<i>E. coli</i> ^b		
		PI	OxyR ⁻	OxyR ⁻ /Tyr ^c
<i>R</i> -(-)-HHMA 8	0.3	0.8	0.6	— ^d
(±)-HHMA	0.3	0.75	0.5	—
aminoalcohol 9	1.0	5	2	—
(±)-MMMA	11.3	—	—	—
DA	0.25	4	1.8	—

^a SH-SY5Y = human dopaminergic neuroblastoma cells. PI = propidium iodide assay: live cells, PI negative; dead cells, PI positive. TC₅₀ in mM. ^b TC₅₀ in μmol/plate. ^c Tyr = 50 units of tyrosinase per plate. ^d (-), survival >50% at the highest dose tested.

Table 2. Mitochondrial Generation of Superoxide Anion by *R*-(-)-HHMA in Comparison with Related Catecholamines

compound	dose (mM)	F.A.U. ^a
—	—	8.0
<i>R</i> -(-)-HHMA 8	0.1	8.0
	0.5	14.8
(±)-HHMA	0.1	8.6
	0.5	13.3
aminoalcohol 9	0.25	11.5
	0.5	13.3
DA	0.1	9.1
	0.31	10.1

^a Mitochondrial generation of superoxide anion was determined by flow cytometry using the MitoSOX Red fluorochrome. FAU = fluorescence arbitrary units.

Table 3. Flow Cytometric Characterization of Cell Death and of Caspase-3 Activity in Treated SH-SY5Y Cells

compound	dose (mM)	apoptotic cells (%) ^a	necrotic cells (%) ^b	caspase-3 activity (%) ^c
—	—	12	23	9
<i>R</i> -(-)-HHMA 8	0.1	10	34	36
	1	14	80	37
(±)-HHMA	0.1	9	30	42
	1	10	82	37
aminoalcohol 9	0.5	9	29	15
	1	15	51	27
(±)-MMMA	10	48	25	18
DA	0.1	13	35	16
	1	11	83	22

^a PI intermediate cells. ^b PI positive cells. ^c Caspase-3 activity was determined by flow cytometry using cleaved caspase-3 (Asp175) antibody.

MMMA. These results were complemented by a flow cytometric measurement of cleaved (activated) caspase-3, a critical effector of most of the apoptotic pathways (Table 3). For *R*-(-)-HHMA and (±)-HHMA, the activity of caspase-3 increased to a maximal value after exposure to 0.1 mM, a dose below the TC₅₀ value (0.3 mM). For aminoalcohol **9** and DA, maximal induction of caspase-3 activity required a higher dose (1 mM), whereas for (±)-MMMA, a significant increase in caspase-3 activity was observed at 10 mM, in the absence of any detectable cytotoxicity. These results suggest that induction of necrosis is dominant over that of apoptosis in ROS-sensitive SH-SY5Y cells. In these cells, induction of proapoptotic events such as caspase-3 activation would not be followed by the detection of apoptosis.

Conclusions

Despite several years of intensive efforts, the mechanisms by which MDMA destroys brain serotonin (5-HT) axon terminals remain to be fully elucidated. In particular, the

sequence order of events and the identity of specific neurotoxic entities have yet to be determined. There has recently been a resurgence of interest in the possibility that MDMA metabolites (especially 5-NAC-HHMA) might play a role in MDMA neurotoxicity. The discrepant findings between the recently published work (19) with those previously reported (20, 21) leave open the possibility that 5-NAC-HHMA may require the presence of MDMA and/or elevated body temperature to be toxic but also raise the question of the chirality of MDMA, which was not considered in previously reported in vivo studies because HHMA, the precursor of 5-NAC-HHMA metabolite, was used as the racemic mixture. In vitro metabolism of MDMA is enantioselective, with a preference for the *S*-enantiomer caused in part by CYP2C19 and CYP2D6-mediated demethylation (23). However, correlation with the in vivo situation is not straightforward because in vivo catecholic phase I metabolites such as HHMA are further metabolized by *O*-methylation and/or glucuronidation/sulfation. Recent investigations have revealed that the *S*-enantiomer of catecholic phase I metabolites was preferably *O*-methylated by catechol-*O*-methyltransferase (COMT) (50), resulting in the accumulation of the *R*-enantiomer. Therefore, the synthesis of *R*-(-)-HHMA, by allowing the synthesis of noticeable amounts of the corresponding diastereomerically pure form of 5-NAC-HHMA metabolite, will permit a comprehensive examination of its participation in the in vivo neurotoxic effects of ecstasy.

The in vitro toxicological study, performed in human neuroblastoma SH-SY5Y cells, revealed similar toxicities for the HHMA racemate and its *R*-enantiomer. The inclusion in this work of an *E. coli* based plate assay, specific for the detection of oxidative toxicity, showed a good correlation between the toxic effects observed both in human and bacterial cells. This correlation led us to conclude that SH-SY5Y cells exhibit a low protection against oxidative toxicity and that the observed cell death in these cells would be mediated by ROS, mainly generated through the redox activity of the generated quinone species. The toxicophore (i.e., the reactive chemical moiety) would be essentially the catechol group, and therefore, the problem of the toxicity of the phase I catecholic metabolites of MDMA would be related to the toxicity induced by other catecholamine compounds, as is the case with DA. Although to a lesser extent, the nature of the alkylamino side chain of catecholamine derivatives also plays a role. As a result, *R*-(-)-HHMA and aminoalcohol **9**, two enantiomeric pure forms, exhibit different cytotoxicity in *E. coli* plate assays. Probably, a physical parameter such as lipophilicity may contribute to the exhaustive toxicity. Accordingly, *R*-(-)-HHMA is at once more toxic (TC₅₀ = 0.75 μmol per plate) and more lipophilic (log *P* = 0.90) than aminoalcohol **9**, for which TC₅₀ = 5 μmol per plate and log *P* = 0.04.

Important, although HHMA racemate and its *R*-enantiomer exhibited close toxicological profiles, no conclusion could be drawn about the enantioselective toxicity. For a complete comparison and evaluation of the enantioselective toxicity of both enantiomers, the synthesis of optically pure *S*-(+)-enantiomer is required. This synthesis is envisioned in our laboratory and will be reported in due course.

The catechol toxicophore is neither present in MDMA, the precursor of HHMA, nor in MMMA for which the two phenolic groups are protected. For MMMA, no toxicity was detected in the bacterial plate assay, whereas, at high doses, toxic effects could be detected in the flow cytometric assay measuring PI uptake. We can then speculate that the toxicity observed with MMMA is not related to increased oxidative stress. Conse-

quently, caution is advised when comparing this toxicity with that induced by the catecholamine derivatives (38). This conclusion can be extended to MDMA, also bearing a protected catechol so that in studies dealing with MDMA toxicity, there is a need to distinguish the toxicity ascribed to MDMA itself from that depending on MDMA biotransformation leading to catechol metabolites such as HHMA and the thioether conjugates.

A general view, including qualitative as well as quantitative changes in toxicity, can be drawn. The parent drug (MDMA) associated with some adverse effects (12) is metabolized to redox active forms such as HHMA, which would induce, in cells endowed with low antioxidant defenses (Table 1), an oxidative toxicity resulting in necrosis (Table 3). These active forms could be further metabolized (e.g., by phase II conjugation reactions) to compounds such as MMMA able to induce a different kind of toxicity resulting in apoptosis (Table 3). This point of view might be considered when evaluating the in vivo situation, in which enantioselective metabolic reactions play a pivotal role.

Acknowledgment. We thank Dr. M.-B. Fleury, Emeritus Professor at the Paris Descartes University, for fruitful discussions. We also thank Carmen Navarro for her technical assistance. This research was made possible thanks to grants MEC (Spain) BIO2007-65662, EC VI FP projects A-Cute-Tox, and LSHB-CT-2004-512051 (to J.E.O.C.), and to the joint financial support of the Mission Interministérielle de Lutte contre la Drogue et la Toxicomanie (MILDT) and the Institut National de la Santé et de la Recherche Médicale (INSERM) (Appel à projets commun 2007 MILDT-INSERM, Recherche sur les drogues et la toxicomanie) (to M.L.) A.F. thanks MILDT together with INSERM for a Ph.D. grant.

Supporting Information Available: Experimental procedures for the determination of enantiomeric excess of compounds **6** and **8**; ^1H and ^{13}C NMR spectra of (\pm)-HHMA, (\pm)-MMMA, and $R(-)$ -HHMA and its synthetic intermediates, together with aminoalcohol derivatives **7** and **9**; analytical HPLC chromatograms of (\pm)-HHMA, (\pm)-MMMA, $R(-)$ -HHMA, and of aminoalcohol **9**. This material is available free of charge via the Internet at <http://pubs.acs.org>.

References

- Milroy, C. M., Clark, J. C., and Forrest, A. R. W. (1996) Pathology of deaths associated with "ecstasy" and "eve" misuse. *J. Clin. Pathol.* *49*, 149–153.
- Walubo, A., and Seger, D. (1999) Fatal multi-organ failure after suicidal overdose with MDMA, "ecstasy": case report and review of the literature. *Hum. Exp. Toxicol.* *18*, 119–125.
- Fineschi, V., Centini, F., Mazzeo, E., and Turillazzi, E. (1999) Adam (MDMA) and Eve (MDA) misuse: an immunohistochemical study on three fatal cases. *Forensic Sci. Int.* *104*, 65–74.
- Cole, J. C., and Sumnall, H. R. (2003) Altered states: the clinical effects of ecstasy. *Pharmacol. Ther.* *98*, 35–58.
- Ricaurte, G. A., and McCann, U. D. (2005) Recognition and management of complications of new recreational drug use. *Lancet* *365*, 2137–2145.
- Green, A. R., Mehan, A. O., Elliot, J. M., O'Shea, E., and Colado, M. I. (2003) The pharmacology and clinical pharmacology of 3,4-methylenedioxymethamphetamine (MDMA, "ecstasy"). *Pharmacol. Rev.* *55*, 463–508, and references therein.
- Lyles, J., and Cadet, J. L. (2003) Methylenedioxymethamphetamine (MDMA, Ecstasy) neurotoxicity: cellular and molecular mechanisms. *Brain Res. Rev.* *42*, 155–168, and references therein.
- Morton, J. (2005) Ecstasy: pharmacology and neurotoxicity. *Curr. Opin. Pharmacol.* *5*, 79–86.
- Baumann, M. H., Wang, X., and Rothman, R. B. (2007) 3,4-methylenedioxymethamphetamine (MDMA) neurotoxicity in rats: a reappraisal of past and present findings. *Psychopharmacology* *189*, 407–424.
- De Win, M. M. L., Jager, G., Booij, J., Reneman, L., Schilt, T., Lavini, C., Olabarriaga, S. D., den Heeten, G. J., and van den Brink, W. (2008) Sustained effects of ecstasy on the human brain: a prospective neuroimaging study in novel users. *Brain* *131*, 2936–2945.
- Gudelsky, G. A., and Yamamoto, B. K. (2008) Action of 3,4-methylenedioxymethamphetamine (MDMA) on cerebral dopaminergic, serotonergic and cholinergic neurons. *Pharmacol., Biochem. Behav.* *90*, 198–207.
- Capela, J. P., Carmo, H., Remiao, F., Lourdes Bastos, M., Meisel, A., and Carvalho, F. (2009) Molecular and cellular mechanisms of ecstasy-induced neurotoxicity: an overview. *Mol. Neurobiol.* *39*, 210–271, and references therein.
- Goni-Allo, B., Puerta, E., Mathuna, B. O., Hervias, I., Lasheras, B., de la Torre, R., and Aguirre, N. (2008) On the role of tyrosine and peripheral metabolism in 3,4-methylenedioxymethamphetamine-induced serotonin neurotoxicity in rats. *Neuropharmacology* *54*, 885–900.
- Esteban, B., O'Shea, E., Camarero, J., Sanchez, V., Green, A. R., and Colado, M. I. (2001) 3,4-Methylenedioxymethamphetamine induces monoamine release, but not toxicity, when administered centrally at a concentration occurring following a peripherally injected neurotoxic dose. *Psychopharmacology* *154*, 251–260.
- Monks, T. J., Jones, D. C., Bai, F., and Lau, S. S. (2004) The role of metabolism in 3, 4-(\pm)-methylenedioxymethamphetamine and 3,4-(\pm)-methylenedioxymethamphetamine (Ecstasy) toxicity. *Ther. Drug Monit.* *26*, 132–136.
- Segura, M., Jordi, O., Farré, M., McLure, J. A., Pujadas, M., Pizarro, N., Llebaria, A., Joglar, J., Roset, P. N., Segura, J., and de la Torre, R. (2001) 3,4-Dihydroxymethamphetamine (HHMA). A major in vivo 3, 4-methylenedioxymethamphetamine (MDMA) metabolite in humans. *Chem. Res. Toxicol.* *14*, 1203–1208.
- Perfetti, X., O'Mathuna, B., Pizarro, N., Cuyas, E., Khymenets, O., Almeida, B., Pellegrini, M., Pichini, S., Lau, S. S., Monks, T. J., Farré, M., Pascual, J. A., Joglar, J., and de la Torre, R. (2009) Neurotoxic thioether adducts of 3,4-methylenedioxymethamphetamine identified in human urine after ecstasy ingestion. *Drug Metab. Dispos.* *37*, 1448–1455.
- Felim, A., Urios, A., Neudörffer, A., Herrera, G., Blanco, M., and LARGERON, M. (2007) Bacterial plate assays and electrochemical methods: an efficient tandem for evaluating the ability of catechol-thioether metabolites of MDMA ("ecstasy") to induce toxic effects through redox-cycling. *Chem. Res. Toxicol.* *20*, 685–693.
- Mueller, M., Yuan, J., Felim, A., Neudörffer, A., Peters, F. T., Maurer, H. H., McCann, U. D., LARGERON, M., and Ricaurte, G. A. (2009) Further studies on the role of metabolites in (\pm)-3,4-methylenedioxymethamphetamine-induced serotonergic neurotoxicity. *Drug Metab. Dispos.* *37*, 2079–2086.
- Jones, D. C., Duvauchelle, C., Ikegami, A., Olsen, C. M., Lau, S. S., de la Torre, R., and Monks, T. J. (2005) Serotonergic neurotoxic metabolites of ecstasy identified in rat brain. *J. Pharmacol. Exp. Ther.* *313*, 422–431.
- Erives, G. V., Lau, S. S., and Monks, T. J. (2008) Accumulation of neurotoxic thioether metabolites of 3,4-(\pm)-methylenedioxymethamphetamine in rat brain. *J. Pharmacol. Exp. Ther.* *324*, 284–291.
- Pizarro, N., de la Torre, R., Joglar, J., Okumura, N., Perfetti, X., Lau, S. S., and Monks, T. J. (2008) Serotonergic neurotoxic thioether metabolites of 3,4-methylenedioxymethamphetamine (MDMA, "ecstasy"): synthesis, isolation and characterization of diastereoisomers. *Chem. Res. Toxicol.* *21*, 2272–2279.
- Meyer, M. R., Peters, F. T., and Maurer, H. H. (2008) The role of human hepatic cytochrome P450 isoenzymes in the metabolism of racemic 3, 4-methylenedioxymethamphetamine and its enantiomers. *Drug Metab. Dispos.* *36*, 2345–2354.
- Anderson, G. M., Braun, G., Braun, U., Nichols, D. E., and Shulgin, A. T. (1978) Absolute Configuration and Psychotomimetic Activity, in *Quasar Research Monograph 22* (Barnett, G., Trisc, M., and Willette, R., Eds.) pp 8–15, National Institute on Drug Abuse, Washington, DC.
- Hiramatsu, M., Nabeshima, T., Kameyama, T., Maeda, Y., and Cho, A. K. (1989) The effect of optical isomers of 3,4-methylenedioxymethamphetamine (MDMA) on stereotyped behavior in rats. *Pharmacol., Biochem. Behav.* *33*, 343–347.
- Johnson, M. P., Hoffman, A. J., and Nichols, D. E. (1986) Effects of the enantiomers of MDA, MDMA and related analogues on [^3H]serotonin and [^3H]dopamine release from superfused rat brain slices. *Eur. J. Pharmacol.* *132*, 269–276.
- Fantegrossi, W. E., Godlewski, T., Karabenick, R. L., Stephens, J. M., Ullrich, T., Rice, K. C., and Woods, J. H. (2003) Pharmacological characterization of the effects of 3,4-methylenedioxymethamphetamine ("ecstasy") and its enantiomers on lethality, core temperature, and locomotor activity in singly housed and crowded mice. *Psychopharmacology* *166*, 202–211.

- (28) Pizarro, N., Farré, M., Pujadas, M., Peiro, A. M., Poset, P. N., Joglar, J., and de la Torre, R. (2004) Stereochemical analysis of 3,4-methylenedioxymethamphetamine and its main metabolites in human samples including the catechol-type metabolite (3,4-dihydroxymethamphetamine). *Drug Metab. Dispos.* 32, 1001–1007.
- (29) Fantegrossi, W. E. (2008) In vivo pharmacology of MDMA and its enantiomers in rhesus monkeys. *Exp. Clin. Psychopharmacol.* 16, 1–12, and references therein.
- (30) Fantegrossi, W. E., Murai, N., Mathuna, B. O., Pizarro, N., and de la Torre, R. (2009) Discriminative stimulus effects of MDMA and its enantiomers in mice: pharmacokinetic considerations. *J. Pharmacol. Exp. Ther.* 329, 1006–1015.
- (31) Felim, A., Neudörffer, A., Monnet, F. P., and LARGERON, M. (2008) Environmentally friendly expeditious one-pot electrochemical synthesis of bis-catechol-thioether metabolites of ecstasy: in vitro neurotoxic effects in the rat hippocampus. *Int. J. Electrochem. Sci.* 3, 266–281.
- (32) Macedo, C., Branco, P. S., Ferreira, L. M., Lobo, A. M., Capela, J. P., Fernandes, E., de Lourdes Bastos, M., and Carvalho, F. (2007) Synthesis and cyclic voltammetry studies of 3,4-methylenedioxymethamphetamine (MDMA) human metabolites. *J. Health Sci.* 53, 31–42.
- (33) Pizarro, N., de la Torre, R., Farré, M., Segura, J., Llebaria, A., and Joglar, J. (2002) Synthesis and capillary electrophoretic analysis of enantiomerically enriched reference standards of MDMA and its main metabolites. *Bioorg. Med. Chem.* 10, 1085–1092.
- (34) Martínez, A., Urios, A., and Blanco, M. (2000) Mutagenicity of 80 chemicals in *Escherichia coli* tester strains IC203, deficient in OxyR, and its oxyR⁺ parent WP2 *uvrA/pKM101*: detection of 31 oxidative mutagens. *Mutat. Res.* 467, 41–53.
- (35) Morgan, P. H., and Beckett, A. H. (1975) Synthesis of some N-oxygenated products of 3,4-dimethoxyamphetamine and its N-alkyl derivatives. *Tetrahedron* 31, 2595–2601.
- (36) Borgman, R. J., Baylor, M. R., McPhillips, J. J., and Stützel, R. E. (1974) α -Methyl dopamine derivatives. Synthesis and pharmacology. *J. Med. Chem.* 17, 427–430.
- (37) Cannon, J. G., Perez, Z., Long, J. P., Rusterholtz, D. B., Flynn, J. R., Costall, B., Fortune, D. H., and Naylor, R. J. (1979) N-alkyl derivatives of (\pm)- α -methyl dopamine. *J. Med. Chem.* 22, 901–907.
- (38) Milhazes, N., Cunha-Oliveira, T., Martins, P., Garrido, J., Oliveira, C., Rego, A. C., and Borges, F. (2006) Synthesis and cytotoxic profile of 3,4-methylenedioxymethamphetamine (“ecstasy”) and its metabolites on undifferentiated PC12 cells: a putative structure-toxicity relationship. *Chem. Res. Toxicol.* 19, 1294–1304.
- (39) Aubry, S., Pellet-Rostaing, S., and Lemaire, M. (2007) Oxidative nucleophilic substitution (S_NO_X) of the benzylic position as a tunable synthesis of tetrahydroisoquinoline natural alkaloid analogues. *Eur. J. Org. Chem.* 5212–5225.
- (40) Wells, G. J., Tao, M., Josef, K. A., and Bihovsky, R. (2001) 1,2-Benzothiazine 1,1-dioxide P₂-P₃ peptide mimetic aldehyde calpain I inhibitors. *J. Med. Chem.* 44, 3488–3503.
- (41) Tang, S., Martinez, L. J., Sharma, A., and Chai, M. (2006) Synthesis and characterization of water-soluble and photostable L-DOPA dendrimers. *Org. Lett.* 8, 4421–4424.
- (42) Bloom, J. D., Dutia, M. D., Johnson, B. D., Wissner, A., Burns, M. G., Largia, E. E., Dolan, J. A., and Claus, T. H. (1992) (R,R)-5[2-[(3-chlorophenyl)-2-hydroxyethyl]-amino]propyl]-1,3-benzodioxole-2,2-dicarboxylate (CL 316, 243). A potent β_3 -adrenergic agonist virtually specific for β_3 receptors. A promising antidiabetic and antiobesity agent. *J. Med. Chem.* 35, 3081–3084.
- (43) Garcia, E., Arrasate, S., Lete, E., and Sotomayor, N. (2005) Diastereoselective intramolecular α -amidoalkylation reactions of L-DOPA derivatives. Asymmetric synthesis of pyrrolo[2,1-a]isoquinolines. *J. Org. Chem.* 70, 10368–10374.
- (44) Clark, R. D., Berger, J., Lee, C.-H., and Muchowski, J. M. (1987) Synthesis and determination of the absolute stereochemistry of the enantiomers of 3-substituted 1,2,3,4-tetrahydroisoquinolines related to the calcium antagonist verapamil. *Heterocycles* 26, 1290–1302.
- (45) Darzynkiewicz, Z., Juan, G., Li, X., Gorczyca, W., Murakami, T., and Traganos, F. (1997) Cytometry in cell necrobiology: analysis of apoptosis and accidental cell death (necrosis). *Cytometry* 27, 1–20.
- (46) Gomez-Santos, C., Ferrer, I., Santidrian, A. F., Barrachina, M., Gil, J., and Ambrosio, S. (2003) Dopamine induces autophagic cell death and α -synuclein increase in human neuroblastoma cells. *J. Neurosci. Res.* 73, 341–350.
- (47) Haque, M. E., Asanuma, M., Higashi, Y., Miyazaki, I., Tanaka, K.-I., and Ogawa, N. (2003) Apoptosis-inducing neurotoxicity of dopamine and its metabolites via reactive quinone generation in neuroblastoma cells. *Biochim. Biophys. Acta* 1619, 39–52.
- (48) Urios, A., LARGERON, M., Fleury, M.-B., and Blanco, M. (2006) A convenient approach for evaluating the toxicity profiles of in vitro neuroprotective alkylaminophenol derivatives. *Free Radical Biol. Med.* 40, 791–800.
- (49) Urios, A., López-Gresa, M. P., González, M. C., Primo, J., Martínez, A., Herrera, G., Escubedo, J. C., O'Connor, J. E., and Blanco, M. (2003) Nitric oxide promotes strong cytotoxicity of phenolic compounds against *Escherichia coli*: the influence of antioxidant defenses. *Free Radical Biol. Med.* 35, 1373–1381.
- (50) Meyer, M. R., and Maurer, H. H. (2009) Enantioselectivity in the methylation of the catecholic phase I metabolites of methylenedioxy designer drugs and their capability to inhibit catechol-O-methyltransferase-catalyzed dopamine 3-methylation. *Chem. Res. Toxicol.* 22, 1205–1211.

TX9003374